*Journal of Superconductivity, Vol. 8, No. 6, 1995*

# Pairing Symmetry and Electrodynamics of Superconducting $YBa_2Cu_3O_{7-\delta}$, $Nd_{1.85}Ce_{0.15}CuO_4$, and Nb

**Dong-Ho Wu,[1] Jian Mao,[1] and Steven M. Anlage[1]**

*Received 6 October 1994*

We experimentally investigate the pairing symmetry and electrodynamics of $YBa_2Cu_3O_{7-\delta}$ (YBCO), $Nd_{1.85}Ce_{0.15}CuO_4$ (NCCO), and Nb by examining the temperature dependence of the penetration depth $\lambda(T)$ and surface resistance $R_s(T)$ in a comparative manner. Using the measured $\lambda(T)$ and $R_s(T)$, we extract the complex conductivity $\sigma = \sigma_1 - i\sigma_2$ for each sample, and the quasiparticle scattering time $\tau(T)$ for the *ab*-plane and *c*-axis in YBCO. While NCCO and Nb show a strong resemblance in their electrodynamic properties, the electrodynamic properties of YBCO are very distinctive from the others. The results suggest that NCCO may have a BCS *s*-wave-like pairing state, while YBCO possibly has an unconventional pairing state. We compare the results on YBCO with the *d*-wave pairing scenario, as well as with other possible theoretical models.

**KEY WORDS:** Surface impedance; pairing symmetry; penetration depth; *d*-wave.

The issue of pairing symmetry is important both for fundamental physics and for the technological application of cuprate superconductors. Many attempts have been made to probe the pairing state by measuring the electrodynamic properties of cuprates. Recent experiments demonstrated that at low temperatures, the temperature dependence of the penetration depth $\lambda_{ab}(T)$ in the *ab*-plane of $YBa_2Cu_3O_{7-\delta}$ (YBCO) and $Bi_2Sr_2CaCu_2O_8$ (BSCCO) does not follow the activated exponential behavior expected of an *s*-wave superconductor [1,2]. Instead, it follows either a quadratic or linear temperature dependence. These results have been interpreted as evidence of a *d*-wave pairing state in the copper–oxygen planes of those materials. However, other recent theories have proposed an alternative interpretation of the results, and the theories further proposed different predictions for the *c*-axis electrodynamic properties of those materials [3,4]. Thus, it is suggested that the *c*-axis surface impedance measurements can put further constraints on the pairing symmetry. Our recent experimental results on *c*-axis penetration depth of YBCO single crystals indicate that the experimental results are not consistent with the alternative theoretical proposals; rather, the results confirm a *d*-wave interpretation, at least in YBCO [5]. Despite the consistent description of the results on YBCO, the experimental results with $Nd_{1.85}Ce_{0.15}CuO_4$ (NCCO) are clearly different from those of YBCO. To provide a better understanding of these experimental results, and the theoretical implications, we examine the temperature dependence of the penetration depth, surface resistance, and the complex conductivity for Nb, NCCO, and YBCO in a comparative manner. Also we discuss other possible theoretical interpretations of the results for these cuprates.

A detailed description of sample fabrication and characterization has been published elsewhere [6]. In brief, YBCO and NCCO single crystals were fabricated by the standard flux method in zirconia and alumina crucibles respectively, and NCCO thin films were fabricated using the pulsed laser ablation technique [7]. Typical sample sizes used in this work are 1 mm × 1 mm × 20 $\mu$m for YBCO single crystals, 2 mm × 2 mm × 10–20 $\mu$m for NCCO crystals, and 2.5 mm × 5.5 mm × 5000 Å for NCCO films. The

[1]Center for Superconductivity Research, Physics Department, University of Maryland, College Park, Maryland 20742-4111.



0896-1107/95/1200-0743$07.50/0 

samples were characterized using ac- and dc-magnetization measurements, dc resistivity measurements, and polarized optical microscopy. Nb samples were prepared by cutting a small piece from a bulk Nb single crystal. The surfaces of each Nb sample were mechanically polished and then etched for a few seconds in an etching solution, and subsequently polished with very fine alumina powder. Resulting Nb samples with typical dimension 1 mm × 1 mm × 30 $\mu$m show clean, smooth, and homogeneous surfaces. Although we have achieved homogeneous NCCO single crystals through a trial and error process of chemical etching and microwave characterization, as-grown NCCO crystals contain a small amount of second-phase material [8]. Because microwave measurements require completely pure single-phase samples (at least near the surface), we were not able to make many reproducible measurements with NCCO single crystals. Hence interpretation of data on NCCO single crystals is limited and does not render information as clear as those from NCCO thin films. For this reason we will discuss NCCO thin film results rather than those from NCCO single crystals to identify the electrodynamics of NCCO.

Microwave measurements are performed in a superconducting Nb cavity where the sample is installed on a sapphire hot finger [6,9]. All the samples discussed here were measured in the same probe in the same manner. The experimental resolution of our cavity perturbation technique is typically $\delta R_s \leq 50\ \mu\Omega$ (at 9.6 GHz) and $\delta\lambda \leq 3$ Å for the sample with dimensions $\sim 1 \times 1\ \text{mm}^2 \times 20\ \mu$m. The surface resistance $R_s$ and the penetration depth $\lambda$ are related to the quality factor Q and the resonant frequency $f_0$ through $R_s(T) \sim \delta(1/Q(T))$ and $\Delta\lambda(T) \sim \delta f_0(T)$ [6,9]. Figure 1 displays normalized $\delta(1/Q)$ vs. temperature for Nb and YBCO crystals and a NCCO thin film. The vertical and horizontal axes of Fig. 1 are normalized in such a way that one can compare the temperature dependence of the surface resistance in a sample-independent manner. Both Nb and NCCO samples are consistent with an exponential temperature dependence for $T/T_c < 0.5$, while the YBCO single crystal shows approximately linear temperature dependence for $T/T_c \leq 0.4$ and a peak at $T/T_c = 0.42$. The behavior of YBCO is anomalous and cannot be reconciled with the conventional BCS $s$-wave model. The same tendency can be found in the normalized frequency shift $\delta\Delta f/\delta\Delta f(T/T_c = 0.5)$ [which is proportional to $\Delta\lambda(T)$] data in Fig. 2, where one can see a strong resemblance between NCCO and Nb samples and an anomalous temperature dependence of $\delta\Delta f/\delta\Delta f(T/T_c = 0.5)$ of YBCO. The data indicate that the penetration depth of YBCO follows a linear temperature dependence for $T/T_c < 0.32$, and over a larger temperature range $\delta\Delta f/\delta\Delta f(T/T_c = 0.5)$ follows a form $\alpha(T/T_c) + \beta(T/T_c)^3$ up to $T/T_c = 0.65$ [5].

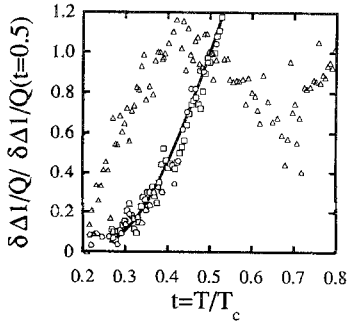


**Fig. 1.** $[\Delta(1/Q(T)) - \Delta(1/Q(t=0.2))]/[\Delta 1/Q(t=0.5) - \Delta 1/Q(t=0.2)]$ [proportional to $R_s(T)$] for $t \equiv T/T_c \leq 0.5$ for NCCO film (squares), Nb single crystal (circles) and YBCO single crystals (triangles). Solid line is an exponential fit mentioned in the text.

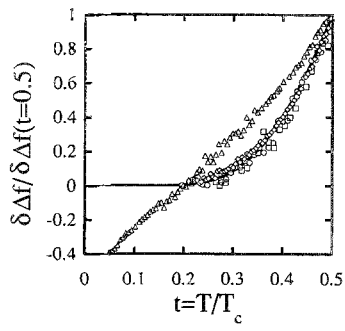


**Fig. 2.** $[\Delta f(t) - \Delta f(t=0.2)]/[\Delta f(t=0.5) - \Delta f(t=0.2)]$ [proportional to $\Delta\lambda(t)$] for $t \equiv T/T_c \leq 0.5$ for NCCO film (squares), NCCO single crystals (diamonds), Nb single crystal (circles), and YBCO single crystals (triangles). Solid line is an exponential fit mentioned in the text.

To make a better comparison of the models with our experimental results, we briefly review the basic features of $s$-wave and $d$-wave pairing states, along with their consequent electrodynamic properties. Figure 3 shows the schematic Fermi surface in $k_{xy}$ space for $s$-wave and $d$-wave states. For the $s$-wave state, a full gap is developed over the Fermi surface and the number of quasiparticles is proportional to $e^{-\Delta_0/k_B T}$ for $T \ll T_c$. Since the electromagnetic absorption (i.e., microwave loss) is proportional to the number of quasiparticles (for $\hbar\omega < \Delta_0$), the surface resistance follows $R_s(T) \propto e^{-\Delta_0/k_B T}$ for $T \ll T_c$. The penetration depth $\lambda(T)$ is a measure of the density of superconducting charge carriers, which is related

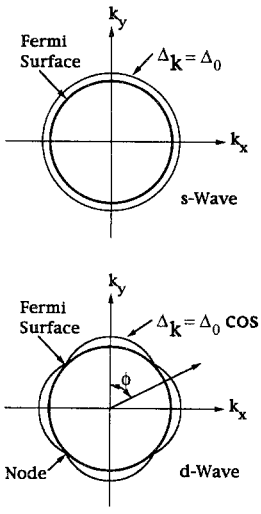


**Fig. 3.** Schematic two-dimensional representations of idealized three-dimensional Fermi surfaces and associated superconducting energy gaps. On the top is a cross section of an idealized spherical Fermi surface with a spherically symmetric energy gap representing an ideal *s*-wave superconductor. On the bottom is a cross section of an idealized cylindrical Fermi surface and a *d*-wave energy gap.

to the number of quasiparticles, so $[\lambda(T)-\lambda(0)]/\lambda(0) \propto e^{-\Delta_0/k_B T}$ for $T \ll T_c$. For the $d_{x^2-y^2}$ state, a gap is developed over the Fermi surface with line nodes running parallel to the axis of the (approximately) cylindrical Fermi surface of the cuprates. The gap has a directional variation in the $k_{xy}$ plane: $\Delta_k = \Delta_0 \cos 2\phi$, where $\phi$ is defined in Fig. 3. Because it is relatively easy to excite quasiparticles at the nodes, the number of quasiparticles is proportional to the temperature $T$. Consequently, $R_s(T) \propto T^2$ and $[\lambda(T)-\lambda(0)]/\lambda(0) \propto T$ for $T \ll T_c$ in a clean *d*-wave superconductor.

With the picture mentioned above, the linear temperature dependence of $\delta\lambda$ has been interpreted as strong evidence of nodes in the quasiparticle excitation spectrum, and also for a *d*-wave pairing state for the hole-doped cuprates. However, there are many alternative theoretical interpretations of this observation. For instance, Kresin and Wolf have proposed an intrinsic .../S/N/S/... multilayer model in which each $CuO_2$ superconducting layer is an *s*-wave superconductor which is proximity coupled to the nominally normal-metal Cu–O chains [10]. This model predicts a linear $T$-dependence of $\delta\lambda$ due to magnetic scattering associated with unpaired spins in the Cu–O chains of oxygen-deficient YBCO [11]. Similarly Klemm and Liu also proposed a model based on an intrinsic proximity effect between *s*-wave layers which can explain the observed temperature dependence of $\lambda_{ab}(T)$ quantitatively [3]. This model further predicts an activated behavior of $\lambda_c(T)$ in YBCO. Since the proposal bears the BCS *s*-wave nature of superconducting layers, and suggests that the linear $T$-dependence of $\lambda_{ab}$ is only a consequence of intrinsic proximity effects between the superconducting layers and normal layers, the test of the behavior of $\lambda_c(T)$ may be used to verify if the pairing state is *d*- or *s*-wave state.

As will be discussed below, our latest experimental results on $\lambda_c(T)$ show a linear temperature dependence at low temperatures, and $\lambda_c(T)$ rapidly increases for $T/T_c > 0.5$ [5]. The results are not consistent with the prediction made by Klemm *et al.*, hence we are forced to rule out at least one model based on the intrinsic proximity effect. Other possible scenarios to explain the linear temperature dependence are models based on an extrinsic proximity effect. In this model, normal metal "dead" layers on the surface of YBCO are proximity coupled to the underlying healthy superconducting material [4]. However, it was found that the properties of the dead layer must resemble those of a very good metal (like Cu or Au) before a $\delta\lambda \sim T$ behavior is seen [4]. Finally, some theorists have proposed that spin-wave excitations can exist in the quasi-two-dimensional $CuO_2$ planes suppressing the condensate density and causing $\delta\lambda \sim T$ at low temperatures [12,13]. However, these spin wave modes are gapped in a superconductor, and thermal energies are orders of magnitude too small to excite such modes. Although these models can give a qualitative description for the temperature dependence of $\lambda(T)$, the models fail when tested quantitatively. Considering all of the available models, our YBCO results are most consistent with the $d_{x^2-y^2}$ model: linear $T$-dependence of $\lambda_{ab}(T)$ and $\lambda_c(T)$ at low temperatures, rapid increase of $\lambda_c(T)$ at $T/T_c > 0.5$ [5], and, moreover, a quantitative agreement on the slope of $\Delta\lambda_{ab}(T)/\Delta T \sim 5$ Å/K [14].

While our results from YBCO support $\Delta\lambda(T) \propto T$ for $T \ll T_c$, we find a linear temperature dependence as well for $R_s(T)$ for $T < 20$ K from several different YBCO samples. This is consistent with the clean *d*-wave model prediction, which says that $R_s(T) \sim T^2$ at low temperatures. It is important to note that the linear temperature dependence of $R_s(T)$ at low temperatures has been seen even in more imperfect YBCO samples. Hence we cannot preclude the possibility of *d*-wave pairing simply because of our observation of linear $T$-dependent $R_s(T)$. To obtain a clearer phenomenological picture about losses in YBCO, we examine the complex conductivity $\sigma = \sigma_1 - i\sigma_2$ [15]. Figure 4 shows the real part of the complex conductivity of YBCO, NCCO, and Nb. The

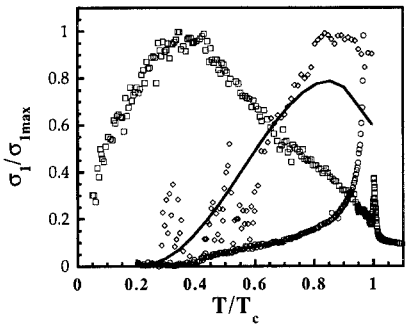


**Fig. 4.** Real part of the complex conductivity $\sigma_1(T)$, normalized to its maximum value $\sigma_{1\max}$, vs. $T/T_c$ for the *ab*-plane of single crystals of YBCO (squares, $\sigma_{1\max}=2.7\times10^7$ $(\Omega\,\mathrm{m})^{-1}$, $T_c=90.1$ K), Nb (diamonds, $\sigma_{1\max}=3.5\times10^8$ $(\Omega\,\mathrm{m})^{-1}$, $T_c=9.2$ K), and an NCCO thin film (circles, $\sigma_{1\max}=3.5\times10^7$ $(\Omega\,\mathrm{m})^{-1}$, $T_c=21.5$ K). The solid line represents a calculated $\sigma_1(T)$ for Nb using the BCS *s*-wave model with gap ratio $2\Delta/k_BT_c\sim4$. The absence of a coherence peak in the NCCO thin film data may be due to the finite thickness effect.

$\sigma_1(T)$ of Nb displays a well-defined BCS *s*-wave coherence peak and overall good agreement with the BCS *s*-wave model. Although the conductivity data from NCCO in general follow the conventional temperature dependence, the coherence peak is not clearly seen in the data, possibly due to the finite thickness effect of the NCCO film [8,16]. The finite thickness ($t$) of the films comes into play when $\lambda\sim t$, modifying the effective surface resistance and reactance of the film. It is precisely in this temperature range that the delicate balance of the bulk $R_s(T)$ and $X_s(T)$ give rise to the coherence peak in $\sigma_1(T)$. Since the corrections to $R_s$ and $X_s$ brought about by the finite thickness can approach 100%, we do not trust a deconvolution of the effective impedance data to determine $\sigma_1(T)$. In contrast to Nb and NCCO samples, the conductivity of YBCO cannot be reconciled with the BCS *s*-wave model. The real part of the conductivity in the *ab*-plane, $\sigma_{1-ab}$, shows a broad peak near $T\sim35$ K, and another sharp peak at the transition temperature. For $T<30$ K, the $\sigma_{1-ab}(T)$ data follow a linear $T$-dependence.

Our data ($\lambda_{ab}$, $R_s$, and $\sigma_{1-ab}$) from YBCO show striking resemblance to what Bonn *et al.* have reported [17]. Interestingly, we found that the conductivity $\sigma_{1-ab}(T)$ of YBCO reported by Gao *et al.* [18] is consistent, at least qualitatively, with ours although their $\sigma_{1-ab}(T)$ was obtained from thin film samples and their $\lambda_{ab}(T)$ and $R_s(T)$ do not resemble ours. Neither peak in our $\sigma_{1-ab}(T)$ is attributed to the coherence effect, rather the peak at $T\sim35$ K has been ascribed to the competition between the unusual rapid increase of the quasiparticle scattering time $\tau$ and the decreasing density of quasiparticles as the temperature decreases [17]. The second sharp peak in $\sigma_{1-ab}$ occurs just below $T_c$ precisely at the point where $\sigma_2=\sigma_1$, and it is not seen in $\sigma_1$ data from Nb [5,16]. The origin of the second peak has not been clearly understood. Our preliminary analysis indicates that the peak may occur both due to the existence of sample inhomogeneity and to fluctuation-enhanced conductivity. Our experiments with various degree of inhomogeneous samples reveal that the second peak becomes sharper as the sample quality improves.

Similar to $\sigma_{1-ab}(T)$, the $\sigma_{1-c}(T)$ data also show a broad peak at $T\sim20$ K [5]. Although both $\sigma_{1-ab}$ and $\sigma_{1-c}$ exhibit a broad peak at low temperatures, their detailed temperature dependences do not appear to be similar to each other. The peak positions are not the same, and, moreover, the overall temperature dependences are not the same. For $\sigma_{1-c}$, the conductivity above the peak increases very slowly until the temperature reaches ~50 K where the conductivity starts to increase rapidly. Also $\sigma_{1-c}(T)$ below the peak appears to show a sublinear temperature dependence. The temperature dependence (both above the peak and below the peak) are not similar to those of $\sigma_{1-ab}$, suggesting that the detailed quasiparticle dynamics in the *ab*- and *c*-directions are different.

A two-fluid interpretation of the *c*-axis conductivity leads to qualitatively similar conclusions as those obtained for the *ab*-plane results by the UBC group [17]. We find that both $1/\tau_{ab}(T)$ and $1/\tau_c(T)$ fall dramatically below $T_c$, although neither clearly follow the $(T/T_c)^3$ form predicted by the *d*-wave model [19], with $1/\tau_{ab}(4.2\,\mathrm{K})\sim10^{11}$ Hz and $1/\tau_c(4.2)\sim3\times10^{11}$ Hz [20]. As Fig. 5 shows, the *ab*-plane scattering rate is better described as $1/\tau_{ab}(T)\sim x_{n,ab}^p$ where $p\sim2.1$–$2.4$ (for *ab*-plane normal fluid fraction $x_{n,ab}>0.25$), and $p<1/2$ (for $x_{n,ab}<0.25$), perhaps indicative of quasiparticle–quasiparticle scattering at high temperatures and residual scattering at low temperatures. Note that the slope of the line in Fig. 5 at high temperatures (corresponding to higher $x_n$) is relatively insensitive to the choice of residual normal fluid fraction, $x_{n0}$. The *c*-axis scattering rate reaches its residual value below about 10 K, and its value is somewhat smaller than a recent far-infrared determination of 85 $\mathrm{cm}^{-1}$ ($\sim2.6\times10^{12}$ Hz) [21]. This low value of the residual scattering rate is consistent with our observation of a "clean-node" $\Delta\lambda_c(T)\sim T$ at low temperatures. It may also mean that nonlocal electrodynamic corrections could

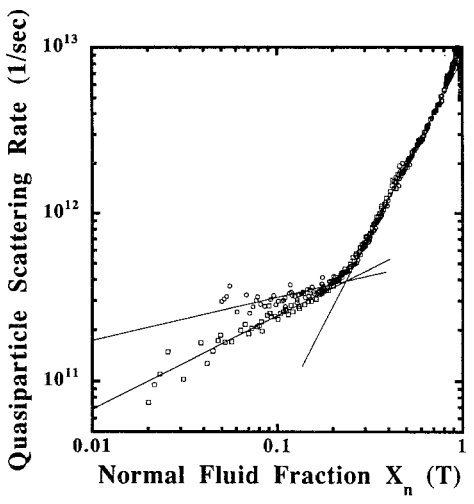


**Fig. 5.** Quasiparticle scattering rate deduced from a two-fluid analysis of the *ab*-plane conductivity data in a YBCO single crystal, plotted vs. the normal fluid fraction in the *ab*-plane. The circles are for a residual normal fraction of 5%, while the squares are for a residual normal fraction of 2% (see [20]). Straight lines are guides to the eye demonstrating the linearity of the data on this log-log plot.

become important in YBCO at low temperatures, as the mean free path approaches the screening length in the *c*-direction.

Our results for $\sigma_{1c}(T)$ and $\lambda_c(T)$ in YBCO are rather different from other recent measurements of *c*-axis properties in related cuprate materials. *s*-Wave-like temperature dependences have been seen in the *c*-axis plasma frequency of $YBa_2Cu_4O_8$ by Basov *et al.*, [22] and in $\lambda_c(T)$ of superconducting $La_{2-x}Sr_xCuO_4$ by Shibauchi *et al.* [23]. The samples measured by Basov *et al.*, had no coherent Drude-like component in the low-frequency conductivity and are thought to be naturally underdoped [22], whereas our samples, like those of Schützmann *et al.* [21], have a metallic *c*-axis conductivity above $T_c$ [5]. Shibauchi *et al.* interpreted their data in terms of a SIS Josephson coupling model for *c*-axis shielding currents, implying that the *c*-axis screening length is really a Josephson penetration depth for an SIS junction. Our *c*-axis screening length temperature dependence more nearly resembles that of a Josephson penetration length for a SNS junction [5]. The low normal-state resistivities of our YBCO crystals [6], along with the low $T_c$ of Schützmann's samples, suggest that both are overdoped. This suggests that the *c*-axis electrodynamic properties may be very sensitive to doping, as well as to the particular layered structure of each cuprate material. It may be that optimally doped and underdoped YBCO will show non-Drude behavior in the *c*-axis low frequency conductivity, and an *s*-wave-like (or SIS-like) temperature dependence to the *c*-axis screening length.

In summary, we have measured the surface impedance of YBCO, NCCO, and Nb samples. While NCCO and Nb are consistent with the BCS *s*-wave behavior, the experimental results from YBCO do not appear to be consistent with the BCS *s*-wave model or related proximity effect models. Rather, we find that the linear temperature dependence of the magnetic penetration depth in the *c*-axis and *ab*-plane confirm a consistent *d*-wave picture with line nodes in the *c*-direction on a cylindrical Fermi surface. Although the detailed quasiparticle dynamics along the *c*-axis are different, the quasiparticle scattering rate decreases dramatically below $T_c$, both in the *c*-axis direction and *ab*-plane. The overall anisotropic surface impedance temperature dependence is not consistent with either intrinsic or extrinsic proximity-effect models, but is consistent with a $d_{x^2-y^2}$ pairing state, except for the linear temperature dependence of $\sigma_1(T)$ and $R_s(T)$ at low temperatures. Our observation with the cuprates yields some conflicting results. Although they are in the same cuprate family, NCCO shows a consistent behavior with the BCS *s*-wave and YBCO is consistent with the *d*-wave behavior. These inconsistencies of experimental observations may suggest that an $s+d$ or $s+id$ wave pairing state, with variable weighting of the two symmetries, may be appropriate for the cuprates.

## ACKNOWLEDGMENTS

We would like to acknowledge our colleagues in the Center for Superconductivity Research, in particular R. L. Greene, T. Venkatesan, J. L. Peng, and S. N. Mao, as well as conversations with R. P. Huebener. This work was supported by the National Science Foundation through grants NSF DMR-9123198 and NSF NYI grant DMR-9258183.

## REFERENCES

1. W. N. Hardy *et al.*, *Phys. Rev. Lett.* **70**, 3999 (1993).
2. Z. Ma *et al.*, *Phys. Rev. Lett.* **71**, 781 (1993).
3. R. A. Klemm and S. H. Liu, *Phys. Rev. Lett.* **74**, 2343 (1995).
4. M. S. Pambianchi, J. Mao, and S. M. Anlage, *Phys. Rev. B* **50**, 13659 (1994).
5. J. Mao *et al.*, *Phys. Rev. B* **51**, 3316 (1995).
6. S. M. Anlage *et al.*, *Phys. Rev. B* **50**, 523 (1994).
7. S. N. Mao *et al.*, *Appl. Phys. Lett.* **64**, 375 (1994).
8. D. H. Wu *et al.*, *Phys. Rev. Lett.* **70**, 85 (1993).

9. S. Sridhar and W. Kennedy, *Rev. Sci. Instrum.* **59**, 531 (1988).
10. V. Z. Kresin and S. A. Wolf, *Phys. Rev. B* **46**, 6458 (1992).
11. S. A. Wolf, private communication.
12. E. Roddick and D. Stroud, *Phys. Rev. Lett.* **74**, 2343 (1995).
13. M. W. Coffey, "Superconducting phase fluctuation contribution to surface impedance," preprint.
14. J. Mao *et al.*, *IEEE Trans. Appl. Supercond.* **5**, 1997 (1995).
15. Our $R_s(T)$ and $\lambda(T)$ data (measured simultaneously on the same sample) are very easily transformed into $\sigma=\sigma_1-i\sigma_2$ using a minimum of assumptions. Bonn *et al.*, [17] emphasized the $R_s$ data in their analysis and had to choose a $T_c$ to make $\sigma_1$ continuous into the normal state. Klein *et al.* [O. Klein, E. J. Nicol, K. Holczer, and G. Gruner, preprint] also have to choose a value of $\sigma_n$, while both make the assumption that $R_s(T>T_c)=X_s(T>T_c)$.
16. J. Mao and S. M. Anlage, "Theory of the surface impedance of superconductors in a resonant cavity," preprint.
17. D. A. Bonn *et al.*, *Phys. Rev. B* **47**, 11314 (1993).
18. F. Gao *et al.*, *Appl. Phys. Lett.* **63**, 2274 (1993).
19. S. M. Quinlan, D. J. Scalpino, and N. Bulut, *Phys. Rev. B* **49**, 1470 (1994).
20. Applying the two-fluid model to the *c*-axis data is problematic because it is not clearly in the clean limit. See D. A. Bonn *et al.*, *Phys. Rev. Lett.* **72**, 1391 (1994). However, we shall assume that $\xi_c/l_{\mathrm{mfp,c}}<1$ at all temperatures, so that the *c*-axis electrodynamics is never in the extreme dirty limit. In the scattering rate analysis, residual normal fluid fractions $x_{n0}$ of 2 and 31% are added for the *ab*-plane and *c*-axis, respectively, to keep $f(\omega t)\leq 1/2$ (see [17]). However, if one uses the constraint that $f(\omega t)$ approaches its low temperature value with zero slope, one finds $x_{n0}$ of 5 and ~50%, respectively.
21. J. Schützmann *et al.*, *Phys. Rev. Lett.* **73**, 174 (1994).
22. D. N. Basov *et al.*, *Phys. Rev. B* **50**, 3511 (1994).
23. T. Shibauchi *et al.*, *Phys. Rev. Lett.* **72**, 2263 (1994).